Bright Blue Emitting Cu-doped Cs$_2$ZnCl$_4$ Colloidal Nanocrystals

Dongxu Zhu[a,b], Valerio Pinchetti[d], Rosaria Brescia[c], Fabrizio Moro[d], Marco Fanciulli[d], Aiwei Tang[a], Ivan Infante*[b,e], Luca De Trizio*[b], Sergio Brovelli*[d], Liberato Manna*[b]

[a] Department of Chemistry, School of Science, Beijing JiaoTong University, Beijing 100044, China

[b] Nanochemistry Department and [c] Electron Microscopy Facility, Istituto Italiano di Tecnologia, Via Morego 30, 16163 Genova, Italy

[d] Dipartimento di Scienza dei Materiali, Università degli Studi di Milano-Bicocca, via R. Cozzi 55, 20125 Milano, Italy

[e] Department of Theoretical Chemistry, Vrije Universiteit Amsterdam, De Boelelaan 1083, 1081 HV Amsterdam, The Netherlands

Supporting Information Placeholder

ABSTRACT: We report here the synthesis of undoped and Cu-doped Cs$_2$ZnCl$_4$ nanocrystals (NCs), in which we could tune the concentration of Cu from 0.7% to 7.5%. According to electron paramagnetic resonance analysis, in 0.7% and 2.1% Cu-doped NCs the Cu ions were present in the +1 oxidation state only, while in NCs at higher Cu concentrations we could detect Cu(II) ions. The undoped Cs$_2$ZnCl$_4$ NCs were non emissive, while the Cu-doped samples had a bright intra-gap photoluminescence (PL) at 2.6eV mediated by band-edge absorption. The PL quantum yield was maximum (~55%) for the samples with low Cu concentration ($\leq$ 2.1%) and it systematically decreased when further increasing the concentration of Cu, reaching 15% for the NCs with the highest doping level (7.5%). Density functional theory calculations indicated that the PL emission could be ascribed only to Cu(I) ions: these ions introduce intra-gap states that promote the formation of self-trapped excitons, through which an efficient emission takes place.

Cs$_2$ZnCl$_4$ is a wide bandgap material of interest for X-ray scintillators, featuring high detection efficiency and timing resolution, thanks to its fast Auger-free luminescence with emission in the ultraviolet spectral region.[1] It has an orthorhombic crystal structure, with disconnected ZnCl$_4^{2-}$ tetrahedra charge balanced by Cs$^+$ cations (Scheme 1).[1b, 2] Cs$_2$ZnCl$_4$ has also been used as a host for Ce^{3+} ions (with a 20% increase of the scintillation light yield)[2a] and for Mn^{2+}, Cu^{2+} and Ni^{2+} ions (as substitutional dopants) to study d-d transitions in M(II) ions in a crystal lattice providing a tetrahedral coordination.[3] Recent studies on the emission properties of Mn(II) ions in tetrahedral coordination have revealed an interest in Mn-doped hybrid organic-inorganic and fully inorganic zinc(II) halide bulk powders, among which also Cs$_2$ZnCl$_4$, as green emitters.[4] Yet, to date, the optical properties of Cs$_2$ZnCl$_4$ on the nanoscale have not been investigated, nor has any doping been attempted.[5] This work aims to fill this gap, and is also motivated by the quest for non-toxic metal halide nanocrystals (NCs) with optical properties comparable to those of Pb-based perovskite NCs.[6] We developed a colloidal synthesis of undoped and Cu-doped Cs$_2$ZnCl$_4$ NCs, and examined their optical properties. Cs$_2$ZnCl$_4$ NCs had a bandgap of 4.8eV and did not exhibit any photoluminescence (PL); the Cu-doped samples exhibited a bright blue emission peaked at 2.65 eV, mediated by band edge absorption; based on density functional theory (DFT) calculations the emission stems from Cu(I) ions, which generate localized intra-gap states leading in turn to emission via self-trapped excitons.

The NCs were synthesized by using octadecene, oleylamine and oleic acid as surfactants, metal acetates as metal precursors, and benzoyl chloride as precursor for the chloride ions (Scheme 1). By varying the Cu/Zn precursors ratio, we prepared Cu-doped Cs$_2$ZnCl$_4$ NCs with Cu amounts ranging from 0.7% to 7.5% (at% with respect to Zn), based on elemental analyses (Table S1 and Figure S1 of the Supporting Information, SI). All the samples were composed of NCs having a parallelepiped shape, with a mean size around 17 nm (Figure 1a,c and S2), and the orthorhombic Pnma Cs$_2$ZnCl$_4$ crystal structure, as revealed by transmission electron microscopy (TEM) and X-ray powder diffraction (XRPD), (Figure 1d and Scheme 1).

Scheme 1. Synthesis of Cs$_2$ZnCl$_4$ and Cu-doped Cs$_2$ZnCl$_4$ NCs
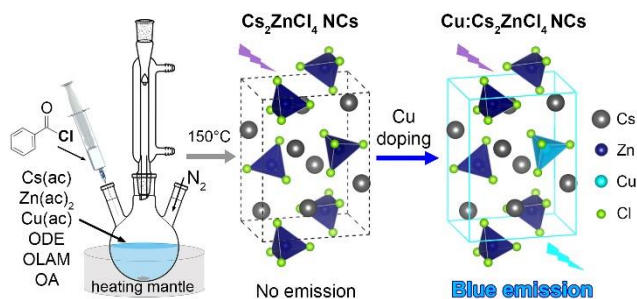
High-resolution TEM (HRTEM) indicated that all products were composed of monocrystalline particles, with a structure matching the orthorhombic Cs$_2$ZnCl$_4$ (Figure 1b and Figure S3), in agreement with the XRPD data. To assess the oxidation state of Cu and Zn in the NCs, we first employed X-ray photoelectron spectroscopy, which however did not provide reliable results, as the NCs degraded quickly under X-ray irradiation. We then performed electron paramagnetic resonance (EPR) spectroscopy on undoped Cs$_2$ZnCl$_4$ NCs and on four Cu-doped Cs$_2$ZnCl$_4$ NC samples, containing 0.7%, 2.1%, 4.3% and 7.5% of Cu, to probe the presence of paramagnetic Cu(II) species (Figure 1e).[7]
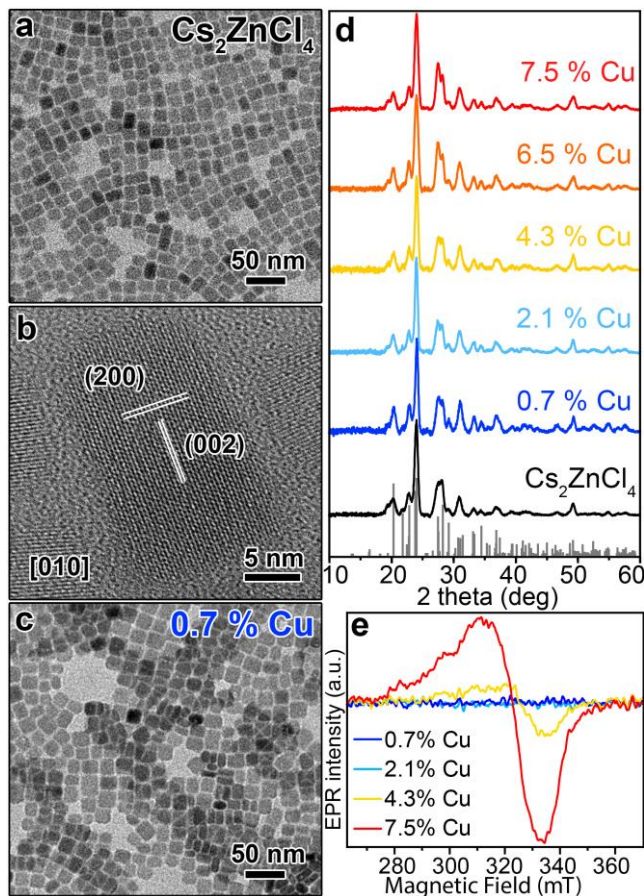
Figure 1. TEM images of Cs_2ZnCl_4 (a) and 0.7% Cu-doped Cs_2ZnCl_4 (c) NCs. (b) HRTEM image of a Cs_2ZnCl_4 NC. (d) XRPD patterns of Cs_2ZnCl_4 and Cu-doped Cs_2ZnCl_4 NC samples with the corresponding bulk reflections (gray bars) of the orthorhombic Cs_2ZnCl_4 crystal structure (ICSD number 6062). (e) EPR powder spectra of Cu-doped Cs_2ZnCl_4 NC samples, having a Cu content of 0.7%, 2.1%, 4.3% and 7.5%, recorded at room temperature.

The EPR spectra of undoped and of both 0.7% and 2.1% Cu-doped Cs_2ZnCl_4 NCs showed no EPR signal, indicating the absence of Cu(II) species, therefore suggesting the presence of diamagnetic Cu(I) ions (Figure 1e). The EPR spectra of 4.3% and 7.5% Cu-doped Cs_2ZnCl_4 NC samples were instead characterized by a signal ascribable to Cu(II) species, as supported by simulations of the low temperature (T=15K) EPR data (of the 4.3% Cu-doped Cs_2ZnCl_4 NC sample, Figure S4). These are compatible with the magnetic resonance transitions of Cu(II) ions (S = ½) and, specifically, with the interactions of their d-electrons with the nuclear spins of the [63,65]Cu (I = 3/2) and the surrounding [35,37]Cl isotopes (I = 3/2, $n.a.$ = 75.78%), (Figure S4).[8] According to EPR data, Cu(II) adopted an axial symmetry within the distorted tetrahedrally coordinated Cl^- anions (*i.e.* occupying Zn(II) sites) (Figure S4).[8a]

Overall, these results indicated that doping of Cs_2ZnCl_4 NCs proceeded via the introduction of Cu(I) ions up to a Cu concentration of 2.1%, above which Cu cations in both +1 and +2 oxidation states were introduced. Since our syntheses were performed under inert atmosphere using a Cu(I) precursor, the formation of Cu(II) cations

is probably due to the disproportionation of Cu(I) ions. The presence of Cu(II) cations as dopants in Cs_2ZnCl_4 is not surprising recalling that Cu(II) doping of bulk Cs_2ZnCl_4 crystals has been already reported.[3b, 3d] The introduction of Cu(I) ions as dopants in Cs_2ZnCl_4 is instead less obvious and had not been reported to date.
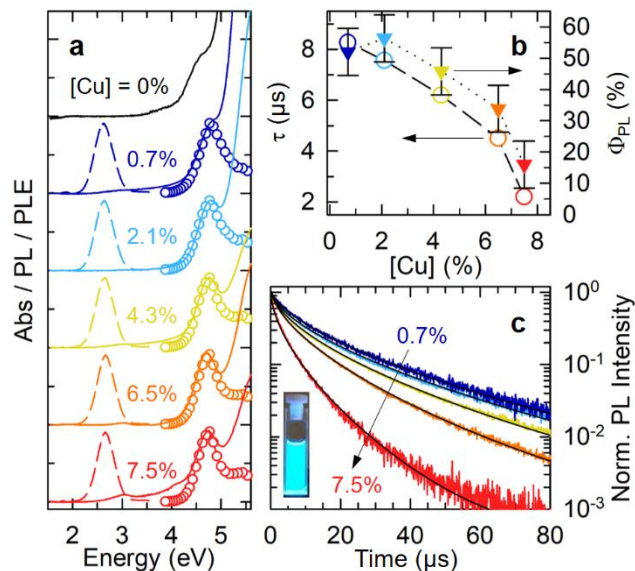

Figure 2. (a) Optical absorption (filled lines), PL (dashed lines) and PLE (empty circles) spectra of undoped and Cu-doped Cs_2ZnCl_4 NCs. (b) Φ_{PL} (filled triangles) and τ (open circles), calculated from the data in (c), as a function of [Cu]. (c) Normalized time-resolved PL decay traces collected at the PL maximum. The black lines are the results of the fitting procedure of the experimental decay curves with a stretched exponential decay function. Inset: photograph of a sample illuminated with 4.9 eV light.

We then investigated the optical properties of undoped and Cu-doped Cs_2ZnCl_4 NCs (Figure 2). The absorption spectra of all the samples featured a main peak at ~4.8 eV, indicating that the introduction of Cu did not modify the main electronic transitions at the band edge (Figure 2a). In the Cu doped NCs there was an additional weak absorption peak at ~3.02 eV (Figure S5) which we ascribed to localized states of Cu(I) ions (see below). Notably, whilst the undoped NCs were not emissive, the addition of Cu led to a bright blue PL at ~2.65 eV (full width at half maximum of 0.45 eV, Figure S6) that was Stokes-shifted from the absorption peak by ~2.15 eV (Figure S7) and by 0.37 eV with respect to the weak absorption at 3.02 eV. The PL excitation (PLE) spectra collected at the emission maximum matched closely the features of the absorption curves: i) a very weak PLE peak ~3.02 eV (see Figure S8); ii) a main peak at ~4.8 eV, indicating that the intragap PL was mostly mediated by band-edge absorption. Both the PL and the respective PLE peak positions were independent on the doping level. In turn, the Cu content had significant impact on the emission quantum yield (Φ_{PL}) that had its maximum value (~55-57±7%) for a Cu concentration of 2.1% and then decreased monotonically to 15±5% for the highest doping level explored (7.5% Cu, Figure 2b). Consistently, time-resolved PL revealed a gradual acceleration of the decay kinetics with oping level (Figure 2c). The PL decay curves were well modeled with a

stretched exponential function $I(t) = I_0 * \exp(-(t/\tau)^\beta)$ that describes the luminescence dynamics of systems featuring a distribution of decay rates due to local structural disorder, as it likely occurs in our NCs due to the different local environments of trapped exciton states. The trend of PL lifetimes (τ) as a function of the Cu concentration followed that of the Φ_{PL} (Figure 2b). Also, the fitting of the PL decay curves yielded a nearly constant stretching factor (β) (Figure S9), suggesting that the local disorder is essentially independent of the Cu-content. This is consistent with the constant PL spectral linewidth of all investigated NCs (Figure S6). The Φ_{PL} and PL lifetime data thus point to the activation of concentration quenching channels, possibly associated with the gradual incorporation of Cu(II) at high doping levels, that compete with the luminescence on the same timescale.

To unravel the origin of the PL emission from the Cu-doped NCs we carried out DFT calculations.[9] First, we computed the band structure of the undoped Cs_2ZnCl_4 system. At the DFT/PBE level of theory,[10] on a 1x1x1 cell, after cell and atomic positions relaxation, we found a direct 4.5 eV bandgap located at the G point (Figure 3a). By expanding the cell to 2x2x2, the gap slightly shrunk to 4.2 eV (Figure 3c), a value lower than the one experimentally observed (4.8 eV, Figure 2a). This discrepancy is expected, as the PBE exchange-correlation (xc) functional typically underestimates the gap.[11] Yet, being PBE computationally cheap, we performed the remaining calculations with this functional, considering a constant underestimation of ~ 0.6 eV, named henceforth as "scissor operator". The band structure of Cs_2ZnCl_4 had two main features: i) the presence of rather localized holes, visible from the flat structure of the valence band region; ii) unlike other 0D systems, such as Cs_4PbBr_6,[12] the conduction band is dispersive, with a marked delocalization of the wavefunction over the 6s orbitals of Cs and the 4s orbitals of Zn, as evinced in the density of states plotted in Figure 3a and 3c, the latter computed at the G point. We then substituted one Zn with a Cu(II) ion in a 2x2x2 cell, which corresponds to a concentration of Cu dopants of 3%. The electronic structure of this system presented a doublet spin-magnetization with broken spin alpha and beta configurations, each identified by up and down arrows in Figure 3d. Here, the bandgap was given by a forbidden d-d transition within the Cu(II) ion calculated at 1.1 eV (Figure 3d). The first allowed transition lied at 4.3 eV, scaled to 4.9 eV by applying the scissor operator (Figure 3d), close to the value of the undoped system (Figure 3c).

These findings suggested that the PL emission of our Cu-doped NCs could not be ascribed to Cu(II) ions, in line with EPR data which indicated the absence of Cu(II) ions in the brightest samples (*i.e.* 0.7% and 2.1% Cu-doped Cs_2ZnCl_4 NCs). To explain the PL mechanism, we computed the band structure of Cu(I) doped Cs_2ZnCl_4 system, obtained by removing a chloride ion from the $CuCl_4$ tetrahedral unit. In this case, the 3d orbitals of Cu moved well inside the bandgap of the Cs_2ZnCl_4 material (Figure 3b). The calculated gap was now 2.2 eV, i.e. 2.8 eV by applying the scissor operator, in line with the presence of a small peak in the absorption and PLE spectra at 3.02 eV , which was, thus, safely ascribed to Cu(I) (Figure 3e).. To observe the evolution of the emissive state, we performed a structural relaxation of the triplet state, which mimics the excited singlet state. The structure of the $CuCl_3$ unit transformed from a planar

geometry, obtained in the ground state of Cs_2ZnCl_4:Cu(I), to a trigonal pyramidal one in the triplet state, pointing to a large structural relaxation. We then computed the electronic structure of the singlet ground state at the geometry of the relaxed triplet (Figure 3f). The gap in this configuration lied at 1.9 eV, 2.5 eV after the scissor operator correction, in line with the observed PL emission (2.65eV, Figure 3f and 2a). Notably, the lowest state of the conduction band was strongly localized on the $CuCl_3$ unit, unlike the ground state conduction band (Figure 2d and S10), suggesting that the exciton becomes self-trapped (consistent with the slow decay time observed experimentally) and providing a gateway for an efficient emission.
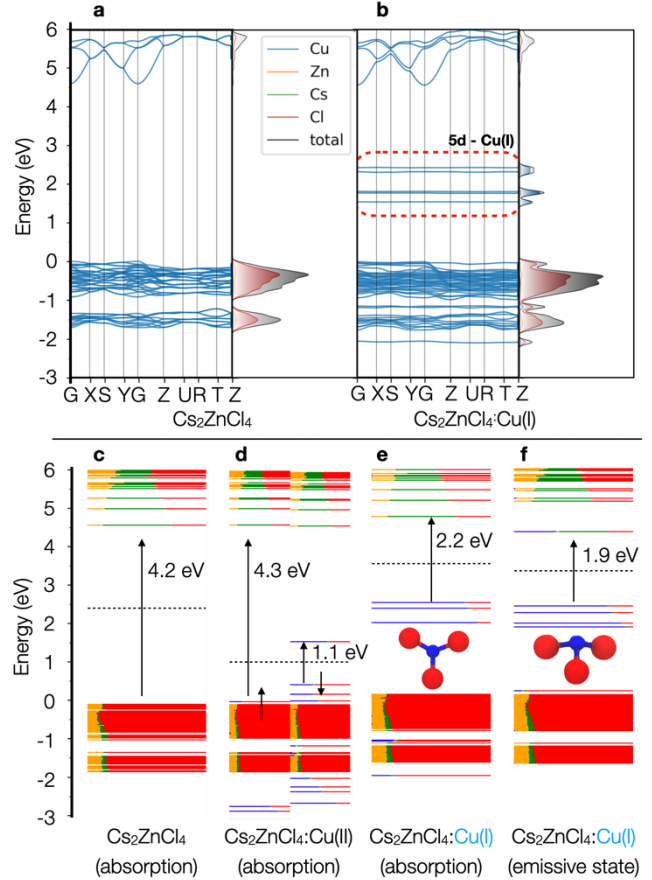

Figure 3. Band structure of (a) pure Cs_2ZnCl_4 and (b) Cs_2ZnCl_4:Cu(I), where one Zn(II) ion was replaced by a Cu(I) ion. Calculations were carried on a 1x1x1 orthorhombic Cs_2ZnCl_4 unit cell. Electronic structure at the G point of a 2x2x2 unit cell computed for (c) Cs_2ZnCl_4, (d) Cs_2ZnCl_4:Cu(II) and (e) Cs_2ZnCl_4:Cu(I). In (e) the reduced Cu(I) was obtained by removing one Cl ion directly attached to Cu, thus formally switching from a tetrahedral $[CuCl_4]^{2-}$ to a trigonal $[CuCl_3]^{2-}$ unit. Cell parameters and ionic positions of all systems were relaxed in the ground state. The electronic structure of the reduced system in (f) was obtained by relaxing cell parameters and ionic position in the triplet state followed by a single-point calculation in the singlet state at this new geometry. This provides a hint on the electronic structure of the emissive state.

In conclusion, we developed a colloidal synthesis of monocrystalline Cs_2ZnCl_4 NCs and doped them with different concentrations of

Cu ions, ranging from 0.7% to 7.5%. The introduction of Cu(I) dopants conferred a bright intra-gap PL emission at 2.6eV to the Cs_2ZnCl_4 NCs which were otherwise non luminescent. The PL quantum yield was maximized (~55%) for the sample with a Cu content of 2.1% and then decreased at higher amounts of dopant. This emission stems from Cu(I) ions introducing intra-bandgap states onto which photo-excited excitons become self-trapped and provide efficient emission. Our findings suggest that a broad range of metal halides, if rationally engineered by doping strategies, may exhibit interesting optical properties and could be employed in photodetectors, scintillators and solar concentrators.

ASSOCIATED CONTENT

Supporting Information

This material is available free of charge via the Internet at http://pubs.acs.org.

SEM-EDS data, TEM and HRTEM images, EPR analysis, Optical data, Molecular orbital plot.

AUTHOR INFORMATION

Corresponding Authors

ivan.infante@iit.it; luca.detrizio@iit.it; sergio.brov-elli@unimib.it; liberato.manna@iit.it

ACKNOWLEDGMENT

REFERENCES

(1)   (a) Yahaba, N.; Koshimizu, M.; Sun, Y.; Yanagida, T.; Fujimoto, Y.; Haruki, R.; Nishikido, F.; Kishimoto, S.; Asai, K., X-Ray Detection Capability of a Cs_2ZnCl_4 Single-Crystal Scintillator. *Appl. Phys. Express* 2014, 7, 062602; (b) Ohnishi, A.; Kitaura, M.; Itoh, M.; Sasaki, M., Electronic Structure and Auger-Free Luminescence in Cs_2ZnCl_4 Crystals. *J. Phys. Soc. Jpn.* 2012, 81, 114704.

(2)   (a) Sugawara, K.; Koshimizu, M.; Yanagida, T.; Fujimoto, Y.; Haruki, R.; Nishikido, F.; Kishimoto, S.; Asai, K., Luminescence and Scintillation Properties of Ce-Doped Cs_2ZnCl_4 Crystals. *Opt. Mater.* 2015, 41, 53-57; (b) McGinnety, J. A., Crystal Structure, Crystal Forces, and Charge Distribution in Salts of the Tetrachlorozincate Anion. *Inorg. Chem.* 1974, 13, 1057-1061.

(3)   (a) Volkov, S. V.; Buryak, N. I., *Russ. J. Inorg. Chem.* 1973, 18, 1260; (b) Sharnoff, M.; Reimann, C. W., Charge-Transfer Spectrum of the Tetrachlorocuprate Ion. *J. Chem. Phys.* 1967, 46, 2634-2640; (c) Weakliem, H. A., Optical Spectra of Ni^{2+}, Co^{2+}, and Cu^{2+} in Tetrahedral Sites in Crystals. *J. Chem. Phys.* 1962, 36, 2117-2140; (d) Valiente, R.; Rodríguez, F., Effects of Chemical Pressure on the Charge-Transfer Spectra of CuX_4^{2-} Complexes Formed in Cu^{2+}-Doped A_2MX_4 (M = Zn, Mn, Cd, Hg; X = Cl, Br). *J. Phys.: Condens. Matter* 1998, 10, 9525-9534.

(4)   (a) Li, Y.; Qi, S.; Li, P.; Wang, Z., Research Progress of Mn Doped Phosphors. *RSC Adv.* 2017, 7, 38318-38334; (b) Morad, V.; Cherniukh, I.; Pöttschacher, L.; Shynkarenko, Y.; Yakunin, S.; Kovalenko, M. V., Manganese(II) in Tetrahedral Halide Environment: Factors Governing Bright Green Luminescence. *Chem. Mater.* 2019, 31, 10161-10169.

(5)   Shamsi, J.; Dang, Z.; Ijaz, P.; Abdelhady, A. L.; Bertoni, G.; Moreels, I.; Manna, L., Colloidal CsX (X = Cl, Br, I) Nanocrystals and Their Transformation to $CsPbX_3$ Nanocrystals by Cation Exchange. *Chem. Mater.* 2018, 30, 79-83.

(6)   (a) Shamsi, J.; Urban, A. S.; Imran, M.; De Trizio, L.; Manna, L., Metal Halide Perovskite Nanocrystals: Synthesis, Post-Synthesis Modifications, and Their Optical Properties. *Chem. Rev.* 2019, 119, 3296-3348; (b) Locardi, F.; Sartori, E.; Buha, J.; Zito, J.; Prato, M.; Pinchetti, V.; Zaffalon, M. L.; Ferretti, M.; Brovelli, S.; Infante, I.; De Trizio, L.; Manna, L., Emissive Bi-Doped Double Perovskite $Cs_2Ag_{1-x}Na_xInCl_6$ Nanocrystals. *ACS Energy Lett.* 2019, 4, 1976-1982; (c) Fu, H., Review of Lead-Free Halide Perovskites as Light-Absorbers for Photovoltaic Applications: From Materials to Solar Cells. *Sol. Energy Mater. Sol. Cells* 2019, 193, 107-132; (d) Ghosh, S.; Pradhan, B., Lead-Free Metal Halide Perovskite Nanocrystals: Challenges, Applications, and Future Aspects. *ChemNanoMat* 2019, 5, 300-312.

(7)   Merks, R. P. J.; Heide, P. v. d.; Beer, R. d., Linear Electric Field Effect on the EPR Spectrum of Single Crystals and Powdered Single Crystals of Cs_2ZnCl_4:Cu^{2+}. *J. Phys. C: Solid State Phys.* 1979, 12, 3097-3104.

(8)   (a) Merks, R. P. J.; De Beer, R., Fourier Transform of The^{133}Cs Modulation of the Electron Spin-Echo Envelope of Cs_2ZnCl_4:Cu^{2+}. *J. Magn. Reson. (1969)* 1980, 37, 305-319; (b) Winter, A.; Zabel, A.; Strauch, P., Tetrachloridocuprates(II)—Synthesis and Electron Paramagnetic Resonance (EPR) Spectroscopy. *Int. J. Mol. Sci.* 2012, 13, 1612-1619; (c) Martini, N.; Parente, J. E.; Toledo, M. E.; Escudero, G. E.; Laino, C. H.; Martínez Medina, J. J.; Echeverría, G. A.; Piro, O. E.; Lezama, L.; Williams, P. A. M.; Ferrer, E. G., Evidence of Promising Biological-Pharmacological Activities of the Sertraline-Based Copper Complex: $(SerH_2)_2[CuCl_4]$. *J. Inorg. Biochem.* 2017, 174, 76-89.

(9)   Hutter, J.; Iannuzzi, M.; Schiffmann, F.; VandeVondele, J., Cp2k: Atomistic Simulations of Condensed Matter Systems. *WIREs Computational Molecular Science* 2014, 4, 15-25.

(10)   Perdew, J. P.; Burke, K.; Ernzerhof, M., Generalized Gradient Approximation Made Simple [Phys. Rev. Lett. 77, 3865 (1996)]. *Phys. Rev. Lett.* 1997, 78, 1396-1396.

(11)   van Meer, R.; Gritsenko, O. V.; Baerends, E. J., Physical Meaning of Virtual Kohn–Sham Orbitals and Orbital Energies: An Ideal Basis for the Description of Molecular Excitations. *J. Chem. Theory Comput.* 2014, 10, 4432-4441.

(12)   Almeida, G.; Ashton, O. J.; Goldoni, L.; Maggioni, D.; Petralanda, U.; Mishra, N.; Akkerman, Q. A.; Infante, I.; Snaith, H. J.; Manna, L., The Phosphine Oxide Route toward Lead Halide Perovskite Nanocrystals. *J. Am. Chem. Soc.* 2018, 140, 14878-14886.